JOURNAL OF MATERIALS SCIENCE 26 (1991) 1395–1400

Surface and grain-boundary energies of cubic zirconia

D. SOTIROPOULOU, P. NIKOLOPOULOS
Institute of Physical Metallurgy, Department of Chemical Engineering, University of Patras, GR-26110 Patras, Greece

Using the multiphase equilibration technique for the measurement of contact angles, the surface and grain-boundary energies of polycrystalline cubic ZrO_2 in the temperature range of 1173 to 1523 K were determined. The temperature coefficients of the linear temperature function obtained, are expressed as

$$\frac{d\gamma}{dT}(ZrO_2) = -0.431 \times 10^{-3} \pm 0.004 \times 10^{-3}\ J\,m^{-2}\,K^{-1}$$

and

$$\frac{d\gamma}{dT}(ZrO_2\text{–}ZrO_2) = -0.392 \times 10^{-3} \pm 0.126 \times 10^{-3}\ J\,m^{-2}\,K^{-1}$$

respectively. The surface fracture energy obtained with a Vickers microhardness indenter at room temperature is found to be $\gamma_F = 3.1\ J\,m^{-2}$.

1. Introduction

The interfacial free energy or interfacial energy is equivalent to the excess Helmholtz free energy per unit area for an interface between different phases, in which one phase is essentially insoluble in the other, or between different orientations in one-component solid materials [1]. In the case of an interface between a condensed phase and a vapour phase or between regions of the same bulk phase with different orientations the interfacial energy is also called surface energy or grain-boundary energy, respectively.

Interfacial energies play an important role in the understanding of phenomena which are related to the production and the properties of new materials. In the consolidation of single as well as multiphase materials by powder technology, the driving force for the sinterability is the reduction of free surface area, with the simultaneous formation of interfacial or grain-boundary area and thus a decrease in the total energy of the system. The microstructure, density, grain-boundary growth or groove penetration by liquids and the mechanical behaviour are influenced by the values of the interfacial energies at the various interfaces of the system.

This paper describes experiments that have been carried out to determine the temperature dependence of the surface and grain-boundary energies of polycrystalline calcia-stabilized zirconia ceramics. The technique employed is multiphase equilibration, which has the advantage of enabling data to be obtained in a wide temperature range (0.4 to 0.9 T_m). Additional data for the surface fracture energy at room temperature are obtained using the Vickers indentation technique.

2. Experimental techniques

2.1. Multiphase equilibration

In order to determine the surface and grain-boundary energies, four sets of experiments are necessary to measure the equilibrium angles that develop at the interface [2, 3]. If torque terms can be neglected [4], then the following equations are valid (Fig. 1):

$$\gamma_{ss} = 2\gamma_{sv}\cos(\psi/2) \quad (1)$$

$$\gamma_{ss} = 2\gamma^*_{sv}\cos(\psi^*/2) \quad (2)$$

$$\gamma_{ss} = 2\gamma_{sL}\cos(\phi/2) \quad (3)$$

$$\gamma^*_{sv} = \gamma_{sL} + \gamma_{LV}\cos\theta \quad (4)$$

where ψ, ψ^* = groove angles, ϕ = dihedral angle, θ = contact angle and γ_{sv}, γ^*_{sv} = surface energies, γ_{ss} = grain-boundary energy, γ_{sL} = interfacial energy.

Experimentally, the groove angles ψ and ψ^* were measured by thermal etching of grain-boundaries in a non-adsorbing gas atmosphere (Fig. 1a) and in an atmosphere contaminated with metal vapour (Fig. 1b), respectively. The dihedral angle ϕ was measured in the presence of a liquid metal phase (Fig. 1c) and the contact angle θ was measured with the aid of the sessile drop technique (Fig. 1d).

Rearranging Equations 1 to 4 the following equations are obtained:

$$\gamma_{sv} = \gamma_{LV}\cos\theta\frac{\cos(\psi^*/2)\cos(\phi/2)}{\cos(\psi/2)[\cos(\phi/2) - \cos(\psi^*/2)]} \quad (5)$$

and

$$\gamma_{ss} = 2\gamma_{LV}\cos\theta\frac{\cos(\psi^*/2)\cos(\phi/2)}{\cos(\phi/2) - \cos(\psi^*/2)} \quad (6)$$

0022–2461/91 $03.00 + .12

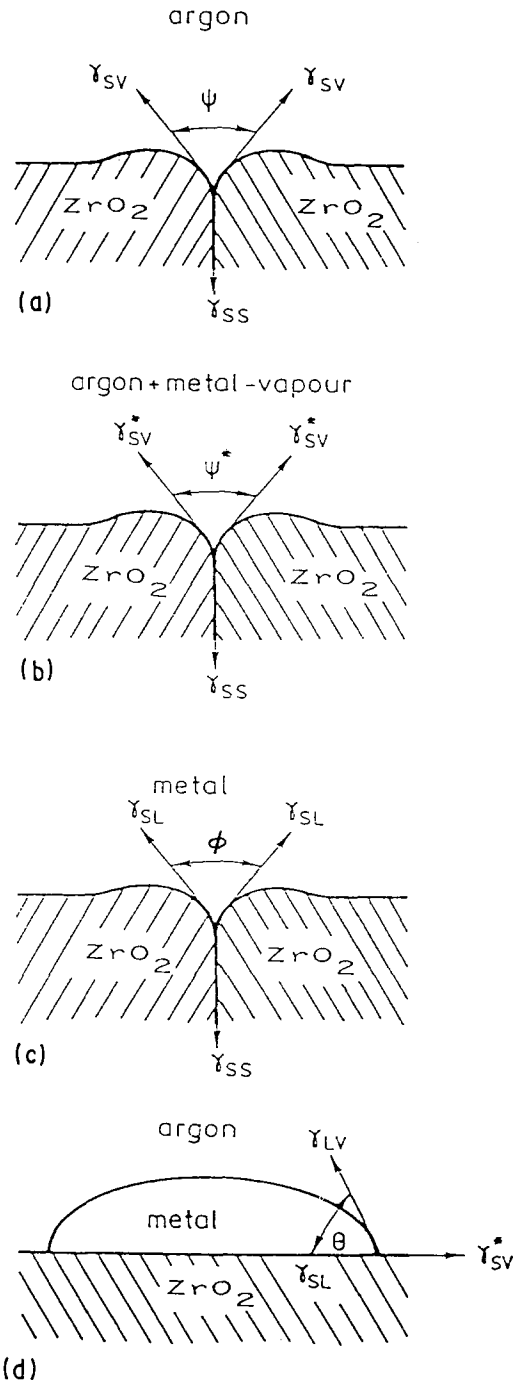

Figure 1 Schematic diagram for a solid–liquid–vapour system in equilibrium showing groove (ψ, ψ^*), dihedral (ϕ) and contact (θ) angles: (a) $\gamma_{SS} = 2\gamma_{SV}\cos(\psi/2)$, (b) $\gamma_{SS} = 2\gamma^*_{SV}\cos(\psi^*/2)$, (c) $\gamma_{SS} = 2\gamma_{SL}\cos(\phi/2)$, (d) $\gamma^*_{SV} = \gamma_{SL} + \gamma_{LV}\cos\theta$.

For determining these energies the only additional data required are for the surface energy of the liquid metal, which is available in the literature.

2.2. Vickers indentation technique

The surface fracture energy (γ_F) for an ideal brittle solid and for plain stress is given by the equation 7 based on Griffith theory [5]:

$$\gamma_F = \left(\frac{1 - \nu^2}{2E}\right) K_c^2 \qquad (7)$$

where ν = Poisson's ratio, E = Young's modulus and K_c = fracture toughness.

An applied method for the determination of fracture toughness (K_c) in ceramic materials [6] is the Vickers microhardness indentation (sharp indenter) which is simple, rapid and non-destructive. As shown in Fig. 2, cracks emerging from the edges of Vickers diamond indentations are formed in brittle materials at high enough loads [7].

According to Anstis *et al.* [6] the fracture toughness is given by the relation

$$K_c = \delta\left(\frac{E}{H}\right)^{1/2}\frac{P}{c^{3/2}} \qquad (8)$$

where $\delta = 0.016 \pm 0.04$ is a material-independent constant for Vickers-produced radial cracks, H = hardness of materials, P = load and c = length of crack from the centre of the impression.

3. Experimental procedure and results

Polished discs of polycrystalline zirconia ZR 23 (trade-name of Friedrichsfeld Co., W. Germany) stabilized with CaO were used in the experiments. The as-received ZrO_2 had a grain size of 30 to 50 μm and no open porosity. According to the chemical analysis of the producer the zirconia contained, in weight percentage, 93% ZrO_2 + HfO_2, 5 to 6% CaO, 0.3 to 0.5% SiO_2, 0.5 to 1.2% MgO, 0.1 to 0.2% Fe_2O_3, 0.5 to 0.8% Al_2O_3 and 0.1 to 0.2% TiO_2.

Metallic tin (Ventron GmbH, W. Germany) was of high purity (≥ 99.9985 wt %). As indicated by chemical analysis, it had a very low oxygen concentration (0.0030 ± 0.0005 wt %). Oxygen as a surface active element is of special interest, since in higher concentrations it lowers the surface energies of liquid metals as well as the interfacial energies between them and a ceramic [8].

Optical interferometry was used to measure the groove angles (ψ, ψ^*) and the dihedral angle (ϕ). Metallographically polished samples were thermally etched using an induction coil furnace in one of the following:

(a) A dry argon atmosphere (groove angle ψ).

(b) Argon with a metal-contaminated atmosphere (groove angle ψ^*). A crucible with tin was introduced in the vicinity of the sample in order to provide the desired metal vapour contamination.

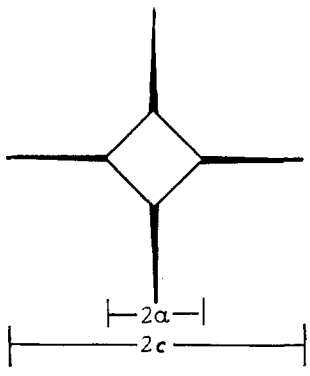

Figure 2 Schematic of Vickers-produced indentation fracture system, showing characteristic dimensions c and α of a radial/median crack and hardness impression, respectively.

(c) For the measurements of the dihedral angle (ϕ), the metal was melted in an argon atmosphere while in contact with ZrO_2. Due to the insufficient wetting, the metal was then removed from the ZrO_2 surface before carrying out the measurements.

The precision of the temperature measurement, carried out with a thermocouple and an optical pyrometer, was found to be $\pm$ 10 K. The true root angles (ψ, ψ^*, ϕ) can be calculated from the apparent root angle α (Fig. 3) with the aid of the following equation [9]:

$$\tan\frac{\psi}{2} = \frac{2d}{1.11\,\lambda m}\tan\frac{\alpha}{2} \quad (9)$$

where d = width between the groove shoulders, λ = wavelength of the light source and m = magnification.

Table I shows the measured groove (ψ, ψ^*) and dihedral (ϕ) angles in the temperature range 1173 to 1523 K for an annealing time of 10 h. In general, measured angles increased slightly with increasing temperature.

The last column in Table I shows the values of the product $\gamma_{LV}\cos\theta$, calculated using the results of sessile drop experiments [10]. Assuming that $\gamma_{LV}\cos\theta$ is a linear function of temperature, the following equation is valid:

$$\gamma_{LV}\cos\theta = -0.595 + 0.391 \times 10^{-3}(T - T_m)\,J\,m^{-2} \quad (10)$$
$$R = 0.9574$$

where $T \geq T_m$ = 505 K = melting point of tin.

The linear temperature function of the surface energy of the liquid tin is given as [11]:

$$\gamma_{LV}(Sn) = 0.544 - 0.07 \times 10^{-3}(T - T_m)\,J\,m^{-2} \quad (11)$$

Most of the Vickers indentations are made using a routine hardness testing facility. A Shimadzu microhardness tester type M was employed to produce a radial crack pattern. The loads were restricted to a range over which the indentation patterns remained well defined, at the lower end by the minimum requirement $c \geq 2\alpha$ (Fig. 2) for validity of Equation 8 and at the upper end by chipping of the specimen.

The loads used were 100, 200, 300 and 500 g. The indented surfaces were examined using the built-in optical microscope. The two diagonals of each orthogonal indentation (2α) as well as the diagonal crack traces (c) were measured and their respective mean values were calculated (Fig. 4).

Figure 3 Interference patterns to obtain the groove angle ψ of ZrO_2 in argon (T = 1523 K, t = 10 h, λ = 589 nm, m = 605 ×).

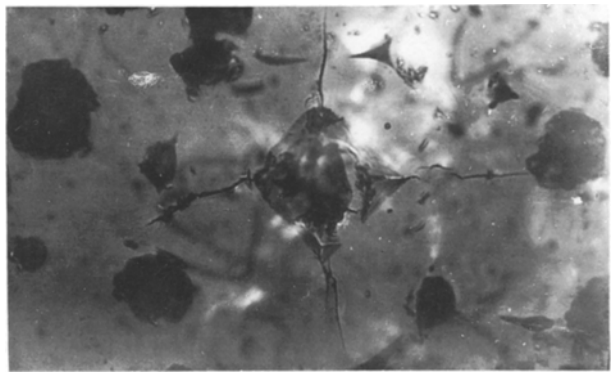

Figure 4 Vickers indentation in ZrO_2 with a load of 500 g (m = 605 ×).

The Vickers hardness number H_V was then calculated from the relation

$$H_V = 18191.6\frac{P}{d^2}\,N\,mm^{-2} \quad (12)$$

where P = load (g) and $d = 2\alpha$ = mean diagonal of indentation (μm). The fracture toughness and the surface fracture energy were calculated using Equations 8 and 7, respectively. The Young's modulus was taken from the specifications of the supplier of ZrO_2 as $1.6 \times 10^5\,N\,mm^{-2}$ and the Poisson's ratio as $\nu = 0.279$ [12]. All the measured and derived values are shown in Table II.

The mean value of K_c (Table II) was found to be $1.04\,MN\,m^{-3/2}$, which compares well with the fracture toughness of yttria-stabilized cubic zirconia single crystals ($\leq 1.7\,MN\,m^{-3/2}$) [13] and magnesia-stabilized cubic zirconia after two hours ageing time at 1373 K ($\sim 1.0\,MN\,m^{-3/2}$) [14], respectively. Furthermore, the fracture toughness of zirconia partially stabilized with magnesia, for a crack radius of 100 μm, is given as about $1.4\,MN\,m^{-3/2}$ [15].

TABLE I Groove angles (ψ, ψ^*), dihedral angle (ϕ), with median standard errors and product $\gamma_{LV}\cos\theta$

T (K)	ψ (deg)	Angles[a]	ψ^* (deg)	Angles[a]	ϕ (deg)	Angles[a]	$\gamma_{LV}\cos\theta$ ($J\,m^{-2}$)
1173	149.20 ± 1.40	45	146.05 ± 0.75	45	155.90 ± 0.58	55	− 0.334 ± 0.031
1373	149.04 ± 0.72	64	148.00 ± 1.03	56	155.82 ± 1.21	11	− 0.256 ± 0.046
1523	153.90 ± 0.42	75	153.95 ± 0.75	41	159.31 ± 0.34	41	− 0.197 ± 0.058

[a] Number of measured groove and dihedral angles.

TABLE II Measured and derived parameters of indentation fracture of zirconium dioxide

Load, P(g)	Hardness impression, 2α(μm)	Hardness, H(GPa)	Radial crack, c(μm)	Toughness, K_c(MN m$^{-3/2}$)	Surface fracture energy, γ_F(J m^{-2})
100	12.86 ± 0.06	10.93 ± 0.02	14.95 ± 1.05	1.039 ± 0.007	3.11 ± 0.04
200	18.22 ± 0.04	10.99 ± 0.02	23.83 ± 0.11	1.030 ± 0.007	3.06 ± 0.04
300	22.14 ± 0.06	11.17 ± 0.03	31.04 ± 0.16	1.030 ± 0.008	3.06 ± 0.05
500	29.40 ± 0.08	11.05 ± 0.05	43.46 ± 0.19	1.042 ± 0.007	3.13 ± 0.04

4. Surface and grain-boundary energies

From the experimental results and the values of the expression $\gamma_{LV} \cos\theta$ shown in Table I the surface energy (γ_{SV}) as well as the grain-boundary energy (γ_{SS}) of ZrO_2 can be calculated using Equations 5 and 6, respectively. The results obtained are shown in Table III.

Fig. 5 shows the calculated values of the surface energy of ZrO_2 as a function of temperature. In the temperature range covered the value of $\gamma_{SV} = 0.84\ J\,m^{-2}$ at 1500 K, calculated by theoretical treatment [10], is in good agreement with the results. If the surface energy is assumed to be a linear function of temperature, the temperature coefficient is given as

$$\frac{d\gamma_{SV}}{dT} = -0.431 \times 10^{-3} \pm 0.004 \times 10^{-3}\ J m^{-2} K^{-1} \quad (13)$$

$$1173\ K \leq T \leq 1523\ K$$

The absolute value of the temperature coefficient derived above is higher than that used up to now for ionic-bonded materials ($-0.1 \times 10^{-3}\ J m^{-2} K^{-1}$). The value of $-0.431 \times 10^{-3}\ J m^{-2} K^{-1}$ compares well with the corresponding temperature coefficients of other oxides such as UO_2 (-0.35×10^{-3}) [3] and ThO_2 (-0.24×10^{-3}) [16], which have similar crystal structures.

Linear extrapolation to higher as well as lower temperatures gives:

(i) a value $\gamma_{SV} = 0.513\ J m^{-2}$ at 2123 K, which shows good agreement with the value of $0.59\ J m^{-2}$ in a helium atmosphere reported by Kingery [17];

(ii) a value $\gamma_{SV} = 0.182\ J m^{-2}$ at the melting point of ZrO_2 ($T_m = 2890$ K), which is lower than the value of the surface energy of pure molten ZrO_2 in air ($\gamma_{LV} = 0.43\ J m^{-2}$) reported by Lihrmann and Haggerty [18];

(iii) a value $\gamma_{SV} = 1.181\ J m^{-2}$ at 573 K, which approaches closely the one measured at this temperature for tetragonal ZrO_2 in air by the heat immersion technique ($\gamma_{SV} = 1.1\ J m^{-2}$) [19].

TABLE III Surface (γ_{SV}) and grain-boundary energies (γ_{SS}) and the ratio γ_{SS}/γ_{SV} for ZrO_2

T (K)	γ_{SV} (J m^{-2})	γ_{SS} (J m^{-2})	γ_{SS}/γ_{SV}
1173	0.922 ± 0.132	0.489 ± 0.066	0.530
1373	0.837 ± 0.244	0.447 ± 0.130	0.534
1523	0.771 ± 0.251	0.348 ± 0.113	0.451

Extrapolation to room temperature (295 K) gives the value $\gamma_{SV} = 1.301\ J m^{-2}$, which is lower than the mean value of surface fracture energy $\gamma_F = 3.10\ J m^{-2}$ (Table II) given by the indentation technique. This difference is probably due to the fact that the multiphase equilibration technique refers to values of "thermodynamic" surface energy at high temperatures concerned with a relaxed and often polarized surface. On the other hand, the surface fracture energy relates to an unrelaxed surface at room temperature [20]. Furthermore, deviation from purely elastic behaviour would lead to a higher cracking load and consequently to an over-estimation of γ_F [21].

A study of the Hertzian cracking of ThO_2 [16], which has a similar crystal structure to stabilized ZrO_2, indicated that the surface fracture energy decreases strongly with temperature from $\gamma_F = 3.3\ J m^{-2}$ at 295 K (for an Al_2O_3 indenter) to $\gamma_F = 1.3\ J m^{-2}$ at 660 K. Assuming a similar behaviour of ZrO_2 one expects in the same temperature range (660 K) a value of γ_F about 1.2 to 1.3 J m^{-2}. This is in good agreement with the value $\gamma_{SV} = 1.143\ J m^{-2}$ that results from linear extrapolation of the values of γ_{SV} in Table III. For the entire temperature range between absolute zero and the melting point of ZrO_2 (Fig. 5), the linear temperature function can be expressed as

$$\gamma_{SV} = 1.428 - 0.431 \times 10^{-3} T (J m^{-2}) \quad (14)$$

$$R = 0.99995$$

Fig. 6 shows the calculated values of the grain-boundary energy (Table III) of ZrO_2 as a function of temperature. The literature value $\gamma_{SS} = 0.38\ J m^{-2}$ at 1500 K [10] compares well with the results. Assuming a linear dependence between grain-boundary energy and temperature, the temperature coefficient is given as

$$\frac{d\gamma_{SS}}{dT} = -0.392 \times 10^{-3} \pm 0.126 \times 10^{-3}\ J m^{-2} K^{-1} \quad (15)$$

$$1173\ K \leq T \leq 1523\ K$$

Extrapolation to higher temperature gives a value $\gamma_{SS} = 0.127\ J m^{-2}$ at 2123 K, which is lower than the value given by Kingery [17] ($\gamma_{SS} = 0.265\ J m^{-2}$). This deviation is probably due to the fact that the error in the calculation of linear temperature coefficient is about 30%. Moreover, Chaim *et al.* [22] give a value $\gamma_{SS} = 0.8\ J m^{-2}$ in yttria-stabilized cubic ZrO_2 at 1523 K, based on the measured dihedral angle (ϕ) between tetragonal ZrO_2 precipitate and cubic ZrO_2.

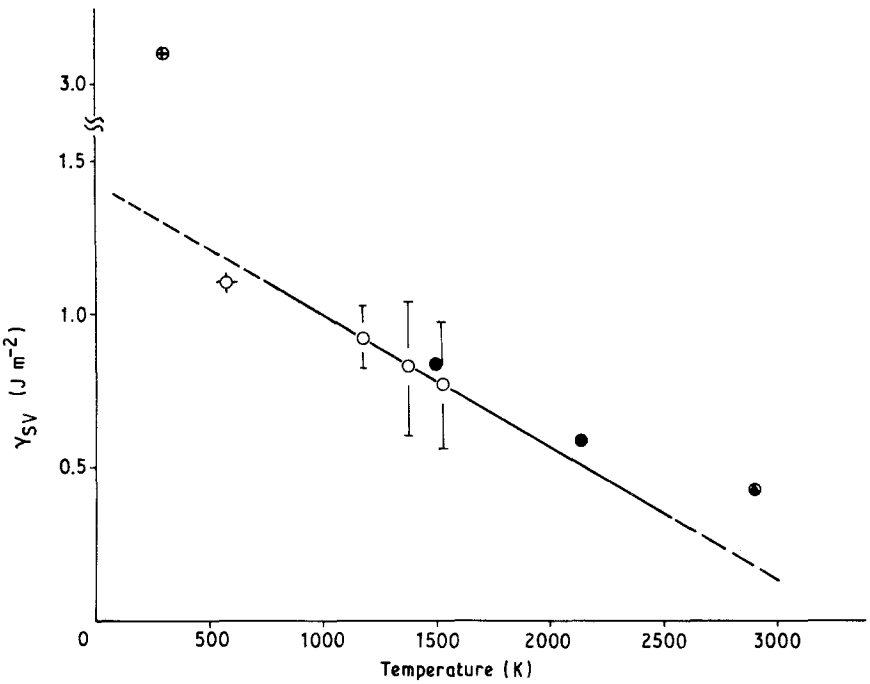

Figure 5 The temperature dependence of the surface energy of ZrO_2. (⊹) Holmes *et al.* (t-ZrO_2) [19]; (●) Nikolopoulos *et al.* [10]; (⊙) Kingery [17]; (▲) Lihrmann *et al.* [18]; (○, ⊕) this work.

The ratio of the grain-boundary energy to the surface energy (γ_{SS}/γ_{SV}) in ZrO_2 varies between 0.45 and 0.53, close to the respective ratio (0.45) of Kingery [17] at 2123 K. As shown by preliminary measurements of groove angles in the temperature region between 1523 and 1923 K, the ratio γ_{SS}/γ_{SV} remains within this range. These ratio values agree reasonably well with values obtained with stoichiometric polycrystalline UO_2 in the same temperature region and a furnace atmosphere (0.53 to 0.58) [3]. Besides calculating the surface and grain-boundary energies it is possible by rearranging Equations 1 to 4 to determine the interfacial energy of the system ZrO_2–Sn from the relation

$$\gamma_{SL} = \gamma_{LV} \cos\theta \frac{\cos(\psi^*/2)}{\cos(\phi/2) - \cos(\psi^*/2)} \quad (16)$$

The resulting values are $\gamma_{SL} = 1.172 \pm 0.144\ J\,m^{-2}$ at 1173 K, $\gamma_{SL} = 1.066 \pm 0.275\ J\,m^{-2}$ at 1373 K and $\gamma_{SL} = 0.969 \pm 0.311\ J\,m^{-2}$ at 1523 K. Assuming a linear temperature dependence of the interfacial energy, the temperature coefficient in the temperature range covered is given as

$$\frac{d\gamma_{SL}}{dT} = -0.577 \times 10^{-3} \pm 0.032 \times 10^{-3}\ J\,m^{-2}\,K^{-1} \quad (17)$$

The metal vapour existing in the furnace atmosphere, as has been shown also in previous work where the Al_2O_3 surface energy was determined [23], does not have a major influence on the surface energy of ZrO_2.

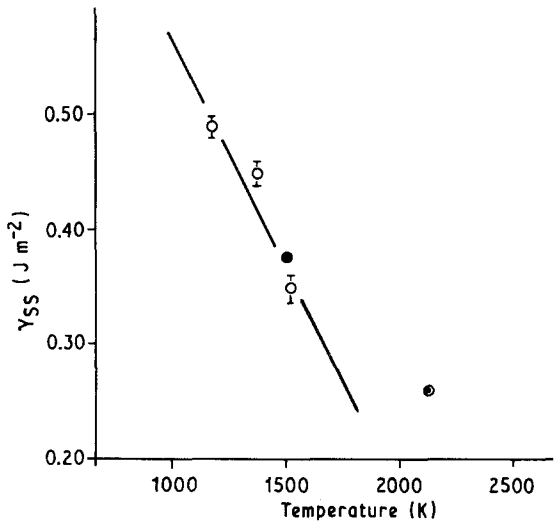

Figure 6 The temperature dependence of the grain-boundary energy of ZrO_2. (⊙) Kingery [17], (●) Nikolopoulos *et al.* [10], (○) this work.

5. Conclusions

The surface and grain-boundary energies of ZrO_2 in the temperature range 1173 to 1523 K were calculated from measurements of equilibrium angles between the phases using the multiphase equilibration technique. The linear temperature coefficients were determined as

$$\frac{d\gamma_{SV}}{dT} = -0.431 \times 10^{-3} \pm 0.004 \times 10^{-3}\ J\,m^{-2}\,K^{-1}$$

for the surface energy and

$$\frac{d\gamma_{SS}}{dT} = -0.392 \times 10^{-3} \pm 0.126 \times 10^{-3}\ J\,m^{-2}\,K^{-1}$$

for the grain-boundary energy. Additionally, the temperature coefficient of the interfacial energy in the ZrO_2–Sn system is given by

$$\frac{d\gamma_{SL}}{dT} = -0.577 \times 10^{-3} \pm 0.032 \times 10^{-3}\ J\,m^{-2}\,K^{-1}$$

The value of the surface fracture energy ($\gamma_F = 3.10\ J\,m^{-2}\,K^{-1}$) obtained with a Vickers microhardness indenter at room temperature is about twice the surface energy (γ_{SV}) calculated by the multiphase

equilibration technique. This difference in the values is probably due to the fact that at room temperature the surface of ZrO_2 is unrelaxed. The values of the surface energy and the surface fracture energy of ZrO_2 are comparable to each other at higher temperature if one assumes that the surface fracture energy of ZrO_2 decreases in the same manner as that of ThO_2.

Acknowledgement

The present work was performed in the framework of a research project financially supported by the Greek Ministry for Industry, Energy and Technology.

References

1. B. C. ALLEN, *J. Less-Common Metals* **29** (1972) 63.
2. E. N. HODKIN and M. G. NICHOLAS, *J. Nucl. Mater.* **47** (1973) 23.
3. P. NIKOLOPOULOS, S. NAZARE and F. THÜMMLER, *ibid.* **71** (1977) 89.
4. B. K. HODGSON and H. MYKURA, *J. Mater. Sci.* **8** (1973) 565.
5. D. BROEK, "Elementary Engineering Fracture Mechanics", (Noordhoff, Leyden, 1974) p. 15.
6. G. R. ANSTIS, P. CHANTIKUL, B. R. LAWN and D. B. MARSHALL, *J. Amer. Ceram. Soc.* **64** (1981) 533.
7. Hj. MATZKE, in "Indentation Fracture and Mechanical Properties of Ceramic Fuels and of Waste Ceramics and Glasses", edited by Hj. Matzke (Harwood, London, 1987) p. 1007.
8. F. A. HALDEN and W. D. KINGERY, *J. Phys. Chem.* **59** (1955) 557.
9. S. AMELINCKX, N. F. BINNENDIJK and E. DEKEYSER, *Physica* **19** (1953) 1173.
10. P. NIKOLOPOULOS, G. ONDRACEK and D. SOTIROPOULOU, *Ceram. Int.* **15** (1989) 201.
11. B. C. ALLEN, in "Liquid Metals", edited by S. Z. Beer (Dekker, New York, 1972) p. 161.
12. R. C. GARVIE, in "Refractory Materials", Vol. 5-II, edited by A. M. Alper (Academic, New York, 1970) p. 157.
13. R. P. INGEL, R. W. RICE and D. LEWIS, *J. Amer. Ceram. Soc.* **65** (1982) C-108.
14. M. V. SWAIN, R. C. GARVIE and R. H. J. HANNINK, *ibid.* **66** (1983) 358.
15. D. B. MARSHALL and M. V. SWAIN, *ibid.* **71** (1988) 399.
16. T. INOUE and Hj. MATZKE, *ibid.* **64** (1981) 355.
17. W. D. KINGERY, *ibid.* **37** (1954) 42.
18. J. M. LIHRMANN and J. S. HAGGERTY, *ibid.* **68** (1985) 81.
19. H. F. HOLMES, E. L. FULLER and R. B. GAMMAGE, *J. Phys. Chem.* **76** (1972) 1497.
20. Hj. MATZKE, *J. Mater. Sci.* **15** (1980) 739.
21. A. G. EVANS and R. W. DAVIDGE, *J. Nucl. Mater.* **33** (1969) 249.
22. R. CHAIM, A. H. HEUER and D. G. BRANDON, *J. Amer. Ceram. Soc.* **69** (1986) 243.
23. P. NIKOLOPOULOS, *J. Mater. Sci.* **20** (1985) 3993.

Received 21 August 1989
and accepted 19 February 1990